Signal Processing Practical

Donald Carr

May 18, 2005

Abstract

This report details the design, implementation and investigation of a range of low pass filters including an active state variable analogue filter, two infinite impulse response digital filters and three finite impulse response digital filters. The report contrasts the expected theoretical frequency response of the filters against the measured response of the filters, and attempts to account for any discrepancies.

1 Introduction

This practical report follows in the wake of a theoretical assignment which had us investigating the design and expected characteristics of a Butterworth low pass filter. Using the Electronic Filter Design HandBook (Williams,1981), we designed two analogue Butterworth filters, sharing a common cutoff frequency but dissimilar topologies. We investigated the circuits using the matrix loop equation, matrix node equation and state variable techniques where appropriate. These all produced a common transfer function, which we investigated using excel and matlab in order to discover its poles, frequency response characteristics and impulse response. We translated the poles of this filter to poles for a digital IIR filter by using the bilinear transformation, for sample frequencies of both 48 kHz and 8 kHz. Using the transfer function skeleton provided by Jonas (2005), we substituted the appropriate poles and obtained a discrete transfer function for each sample frequency. We discovered the poles, frequency response characteristics and unit sample response associated with these transfer functions. We then set about implementing three different FIR digital filters using the rectangular, Hamming and Blackman windowing functions respectively. We calculated forty one coefficients for each filter, and used these to calculate the recurrence relation and subsequently the transfer function for each filter. This transfer function was used within MatLab to determine the z-plane pole zero diagrams and frequency responses for each filter.

Having established frequency responses and appropriate transfer functions for all the filters, we set out to design and implement them and investigate the accuracy of the modelled responses calculated in the assignment.

Theory

Analogue filter

The original transfer function can be separated into two separate transfer functions.

$$
\begin{aligned}
H(s) &= \frac{\frac{\omega_c^3}{2}}{s^3 + 2\omega_c s^2 + 2\omega_c^2 s + \omega_c^3} \\
H(s) &= [\frac{\omega_c}{s+\omega_c}][\frac{\frac{\omega_c^2}{2}}{s^2 + \omega_c s + \omega_c^2}]
\end{aligned}
$$

IIR filters

The original transfer function for the IIR can also be separated into two separate transfer functions.

$$
\begin{aligned}
H(z) &= \frac{(1+z^{-1})^3}{(1-0.1202z^{-1})(1-(0.1595-0.5663i)z^{-1})(1-(0.1595+0.5663i)z^{-1})} \\
H(z) &= [\frac{(1+z^{-1})}{(1-\mathcal{P}_1 z^{-1})}][\frac{(1+z^{-1})^2}{(1-\mathcal{P}_2 z^{-1})(1-\mathcal{P}_3 z^{-1})}] \\
H(z) &= [\frac{(1+z^{-1})}{(1-\mathcal{P}_1 z^{-1})}][\frac{(1+2*z^{-1}+z^{-2})}{(1-(\mathcal{P}_2+\mathcal{P}_3)z^{-1}+\mathcal{P}_2\mathcal{P}_3 z^{-2})}]
\end{aligned}
$$

Procedure

I used a digital oscilloscope for all of my measurements. I made full use of the graphical measurement tools present on the digital oscilloscope to acquire values, removing the haphazard rounding effects inevitable in measuring small wave forms against a scale with the naked eye. I set the oscilloscope to display averaged results, which made the resulting signals incredibly crisp. The filters were all supplied with a sinusoidal wave from a signal generator as input, and the frequency response of all of the resulting filters was roughly measured between 0 and 2500 Hz, though this varied according to the stability of the filtered output at these frequencies.

Analogue filter design

The filter can be physically constructed as 2 separate units due to its separable transfer function. The first unit is a simple passive low pass filter comprised of a resistor and capacitor in series. The second unit, which is adopted from Williams (1981) handles the complex conjugate poles, and is far more sophisticated. Each unit had a general transfer function of its own, and when these transfer functions were equated to the relevant member of the above separated transfer function, they provided components values. This was not required for the circuit acquired from Williams (1981), as the value calculations were already related and simplified in terms of the real and imaginary components of the poles of our filter, and all that was required was the denormalising of these poles by multiplying by our ω_c. These denormalised pole components were then used to calculate our component values. The gain of the original transfer function was calculated to be a half by setting s = 0 in the original transfer function, and this gain was maintained by scaling R4 up by a factor of 2.

When placed in series the units formed a low pass active state variable filter, with Butterworth characteristics.

Component values were calculated :

C	0.01 uF
R4	16k
R2,3	8k
R1	8k
R	1k
Ri	600
Ci	0.132 uF

Table 1: Denormalised values calculated using relations from Williams (1981)

The circuit was built under Microcap initially in order to test the proposed design before attempting physical implementation.

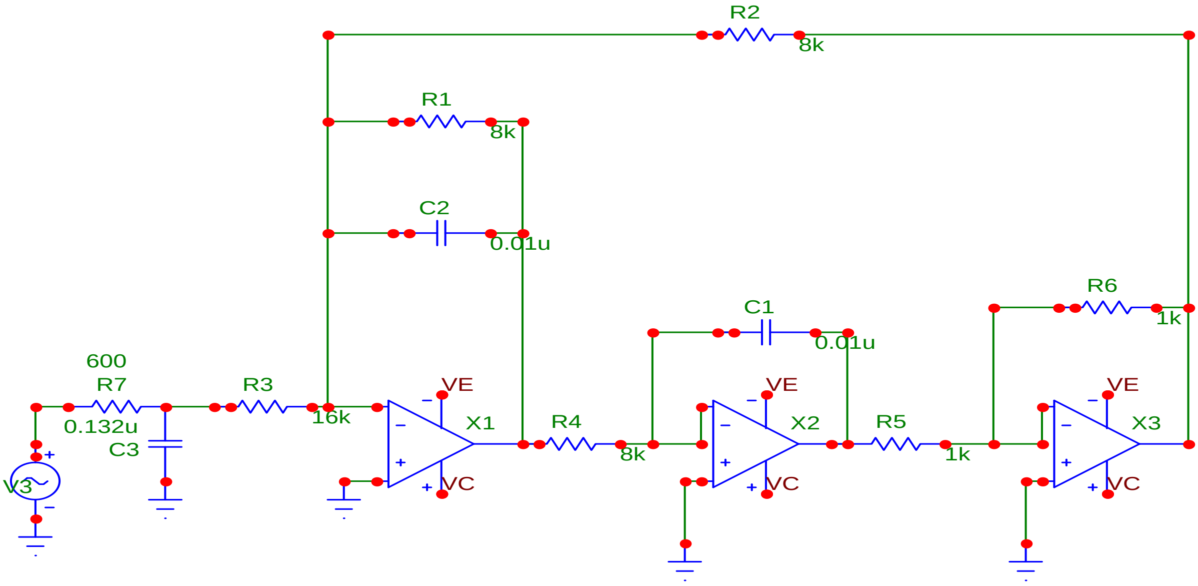

Figure 1: Analogue circuit design

Digital filter design

The digital filters were all to be implemented on a Motorola DSP56002 microchip. Base code was supplied (Appendix 1&2) and we had to familiarise ourselves with the assembly code and subsequently alter it in order to implement the filters correctly.

The source signal was sampled and split into two streams, one of which was filtered and the other left unprocessed. The filtered signal was then compared with the unprocessed signal, rather then the original source, in order to factor in any inherent phase shifting in the operation of the chip.

In an attempt to minimise time wastage, I hit each filter with an impulse from an impulse generator after coding it, in order to check the response of the filter before departing on any frequency response measurement. The filters were also initially probed roughly by rapidly increasing the frequency up from zero in an attempt to spot the obvious Butterworth characteristic of a flat passband and the predicted -3dB drop at ω_c .

IIR digital filter design

The sub routine in Appendix 1 was supplied. The necessary coefficients were calculated using the separable transfer function shown in the IIR theory.

$f_{sample}[Hz]$	$\mathcal{P}_1$	$(\mathcal{P}_2 + \mathcal{P}_3)$	$\mathcal{P}_2\mathcal{P}_3$
8000	0.1202	0.3190	0.3461
48000	0.7685	1.7123	0.7720

Table 2: Matlab generated values for IIR coefficients

These calculated values were halved and then substituted into the code in the appropriate locations.

FIR digital filter design

The sub routine in Appendix 2 was supplied. The necessary coefficients had been calculated previously in the assignment, and were substituted into the code in the appropriate locations. These coefficients had to be normalised to be less then one, as the Motorola chip uses fixed point arithmetic. This was achieved by dividing throughout by a number slightly larger then the largest coefficient and had no impact on the filter design as the ratio between the various coefficients defines the behaviour of the filter.

Results

1.1 Analogue Frequency Response

1.1.1 MicroCap

The frequency response predicted by Microcap is shown below.

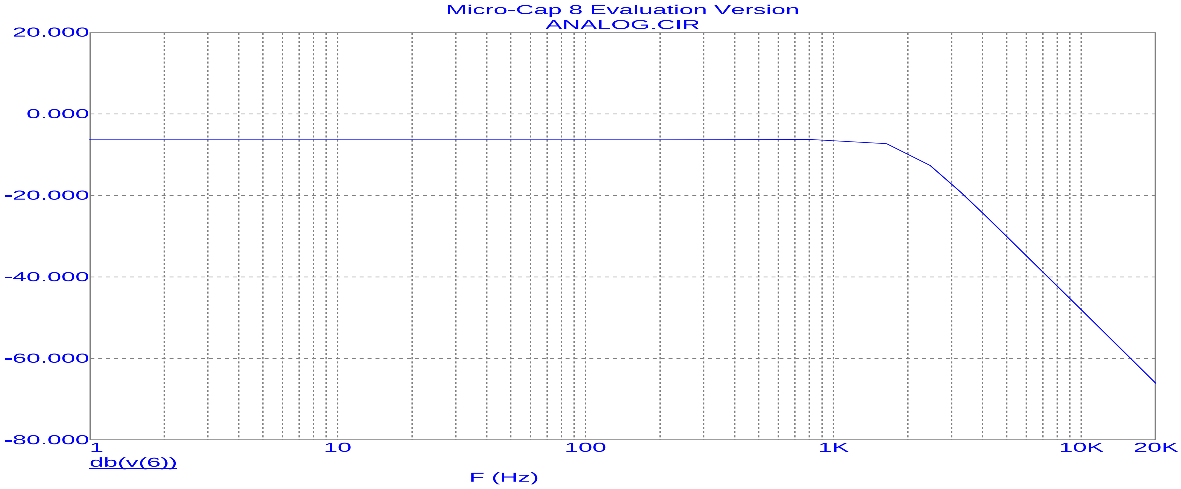

Figure 2: MicroCap bode plot of schematic gain response

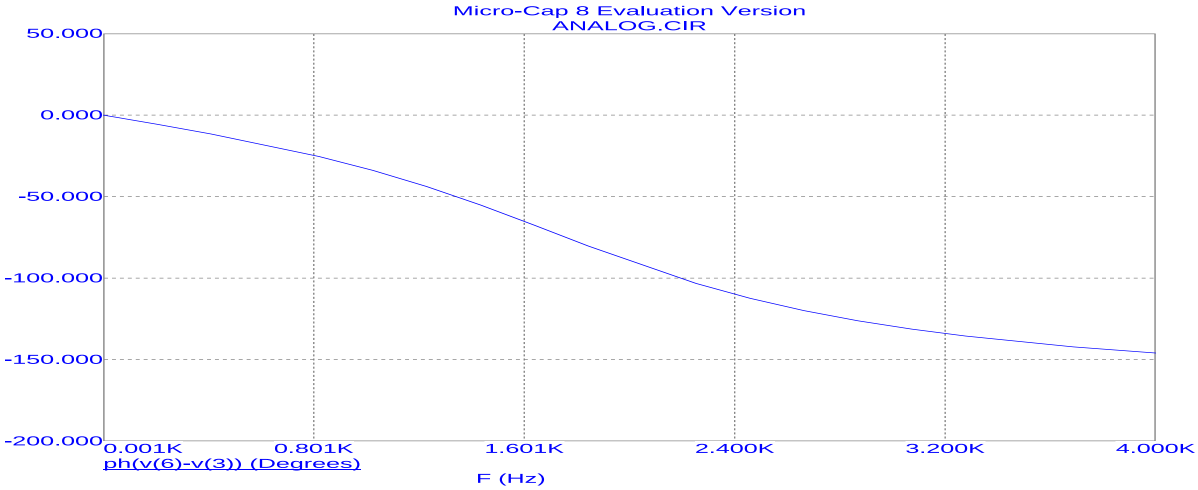

Figure 3: MicroCap plot of schematic phase response

1.1.2 Constructed filter

The measured frequency response of the constructed filter compared to the response predicted for the filter in the assignment, is shown below.

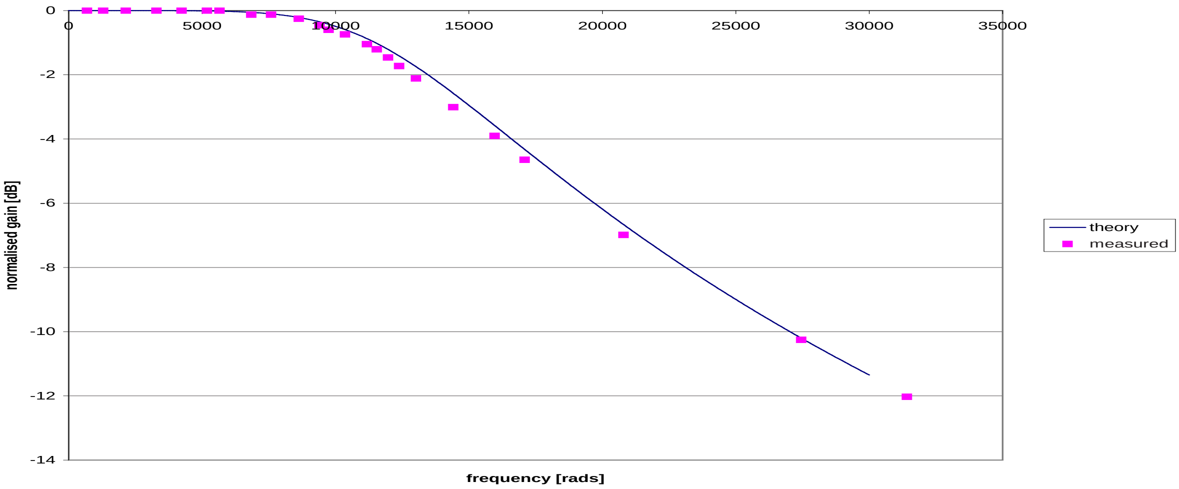

Figure 4: Comparison of theory vs measurements : analogue gain

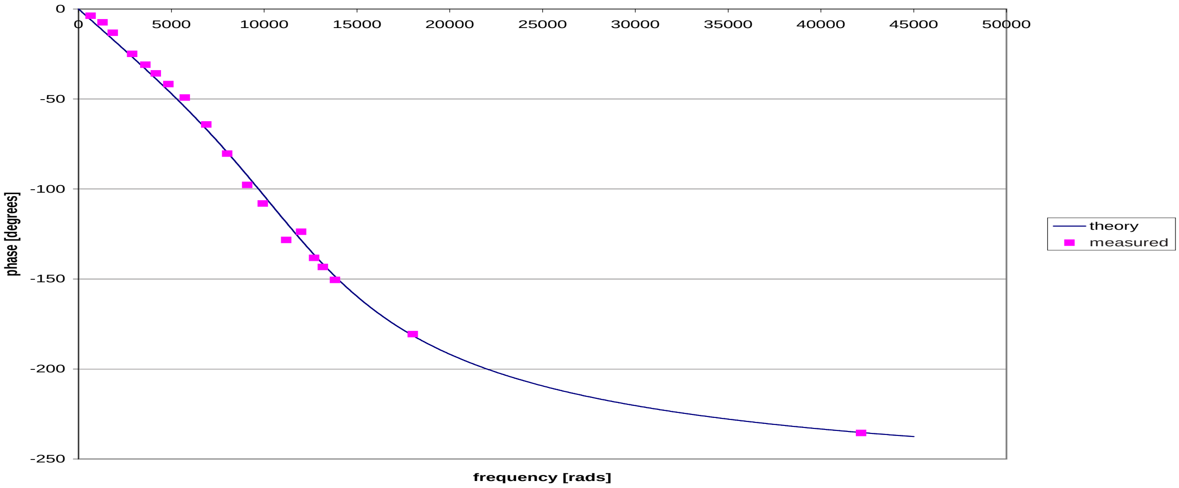

Figure 5: Comparison of theory vs measurements : analogue phase

1.2 Digital Frequency Response

1.2.1 IIR

The measured frequency response of the coded IIR filter compared to the response predicted for the filter in the assignment, is shown below.

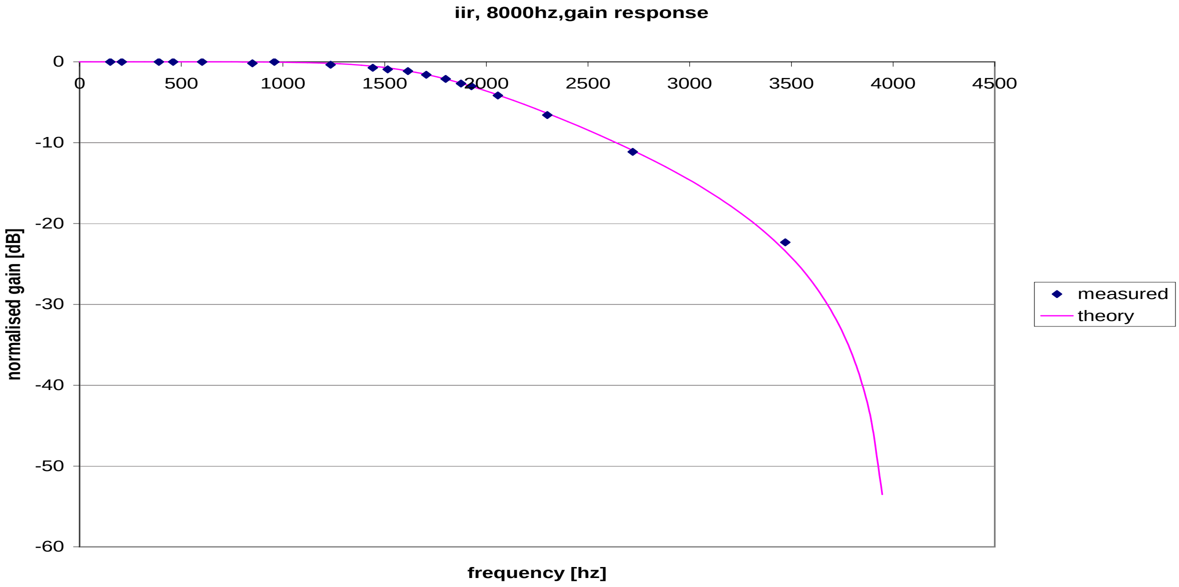

Figure 6: Comparison of theory vs measurements : 8kHz f_{sample} : gain

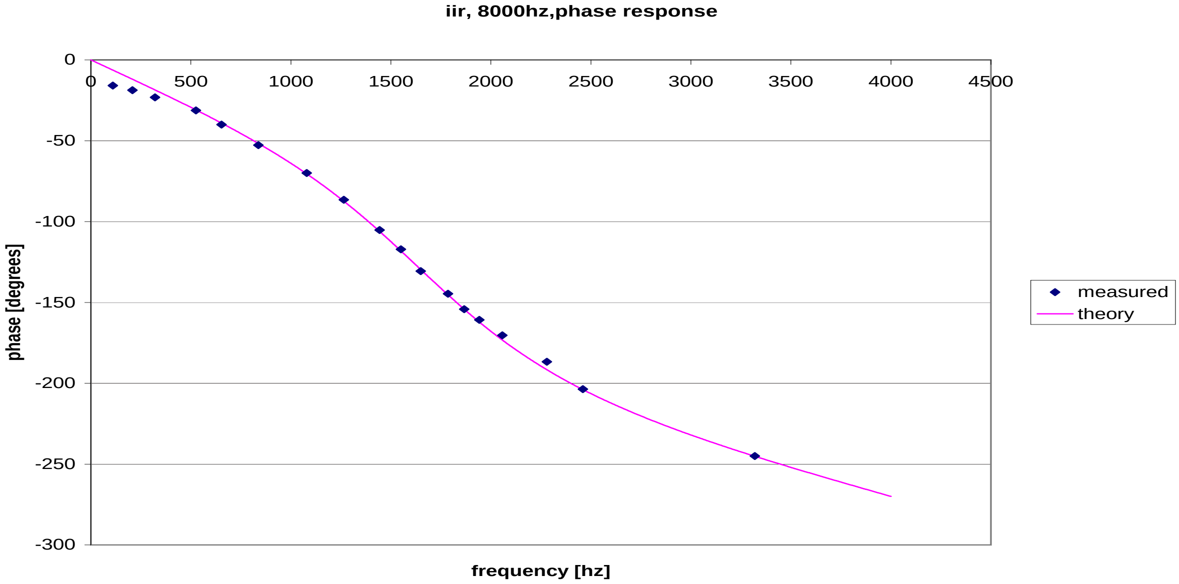

Figure 7: Comparison of theory vs measurements : 8kHz f_{sample} : phase

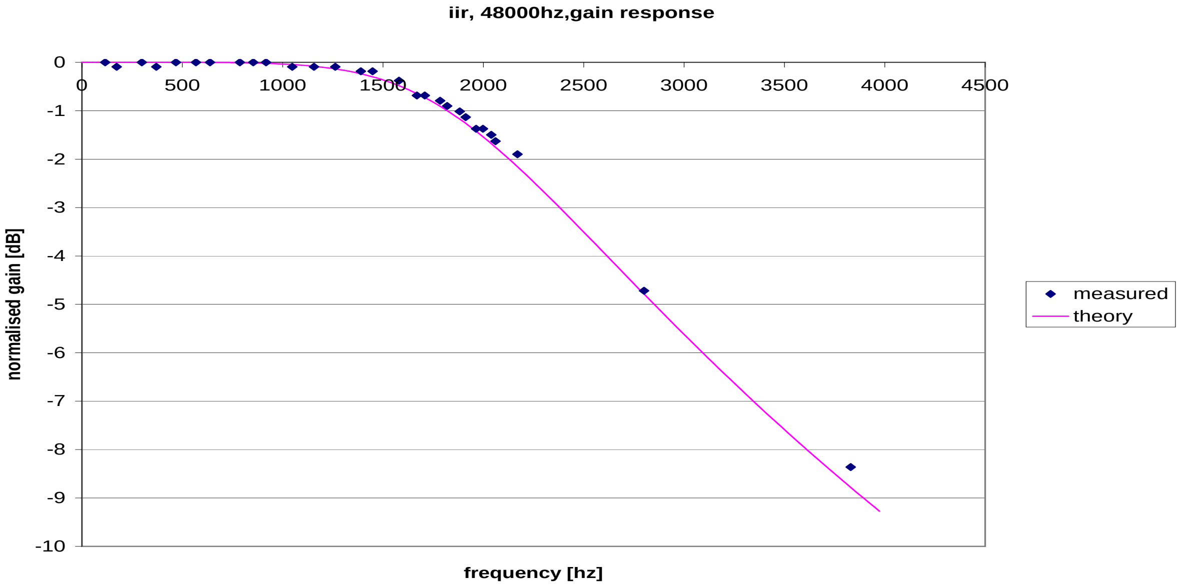

Figure 8: Comparison of theory vs measurements : 48kHz f_{sample} : gain

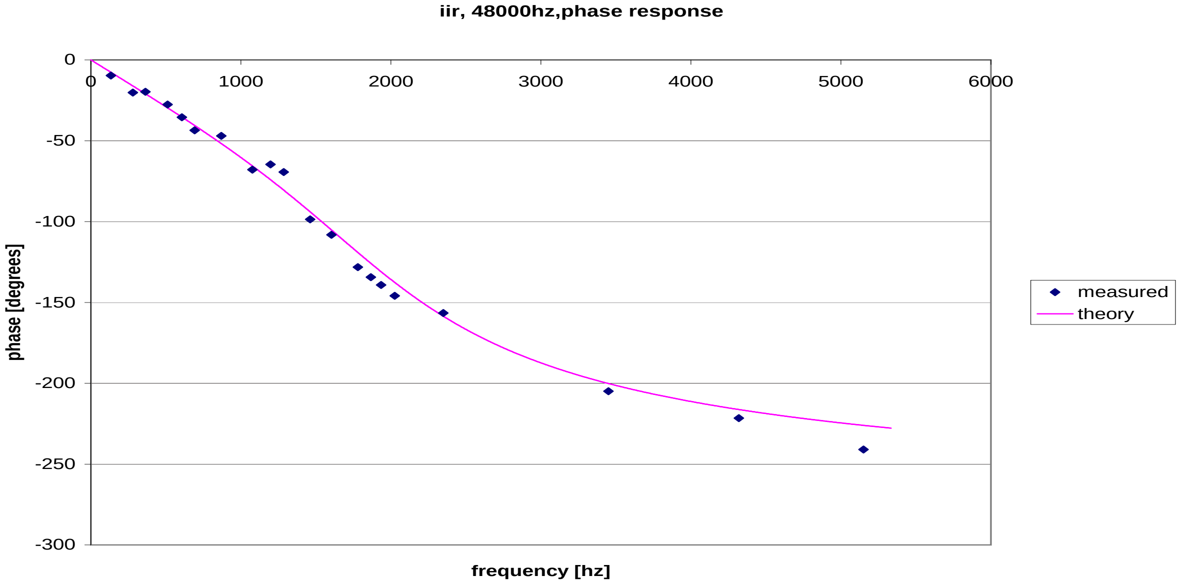

Figure 9: Comparison of theory vs measurements : 48kHz f_{sample} : phase

1.2.2 FIR

The measured frequency response of the coded FIR filter is shown below.

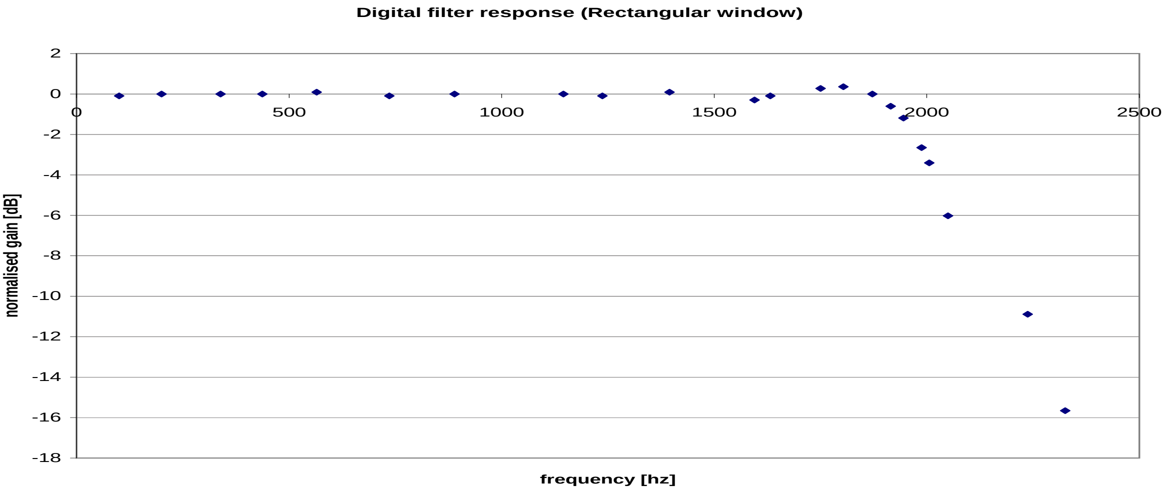

Figure 10: Empirically measured gain response : Rectangular window, f_{sample} 8kHz

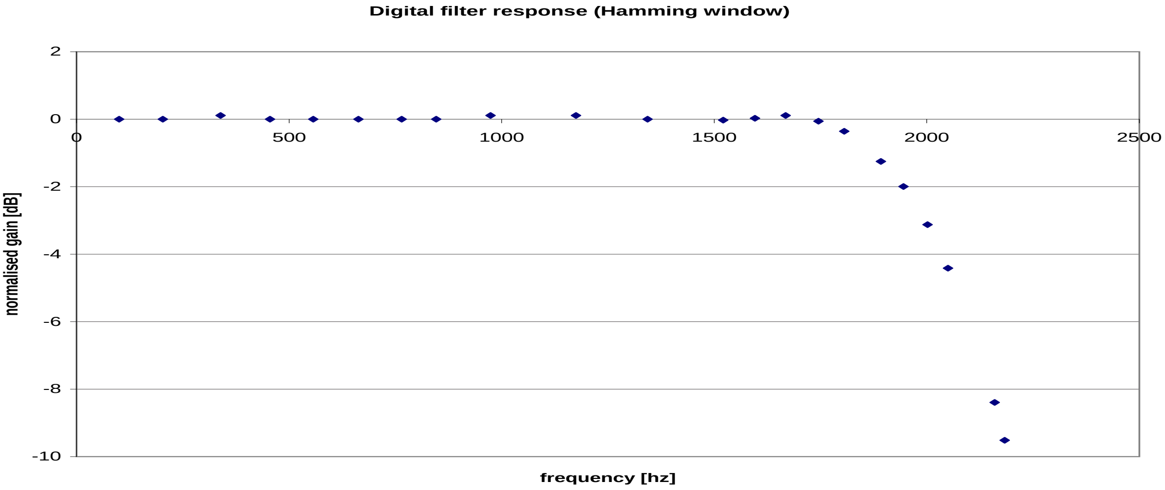

Figure 11: Empirically measured gain response : Hamming window, f_{sample} 8kHz

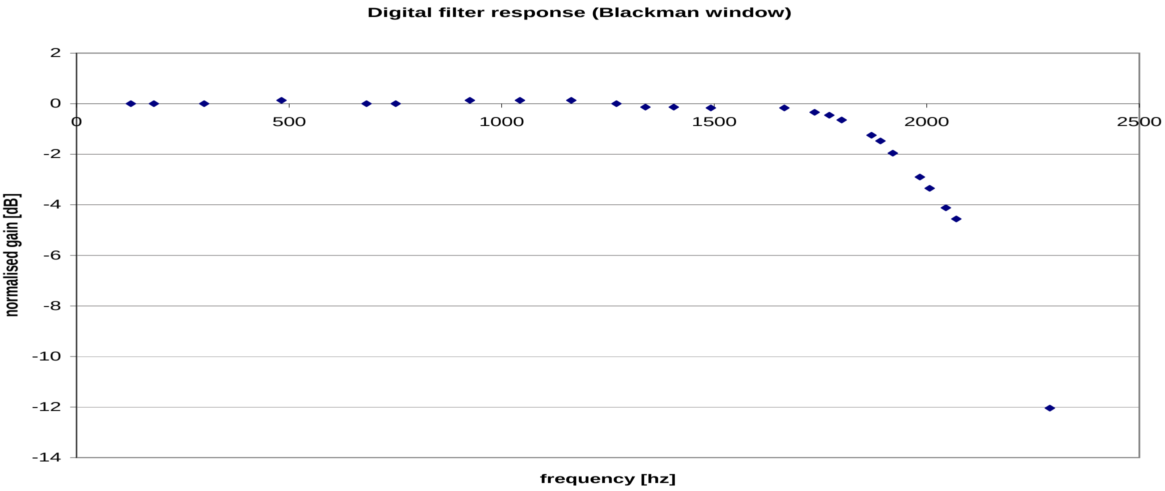

Figure 12: Empirically measured gain response : Blackman window, f_{sample} 8kHz

The measured gain response of the coded FIR filter compared to the response predicted for the filter in the assignment, is shown below. The phase response for all three filters was theoretically almost identical, and these are therefore plotted on one axis with the measured phase shift.

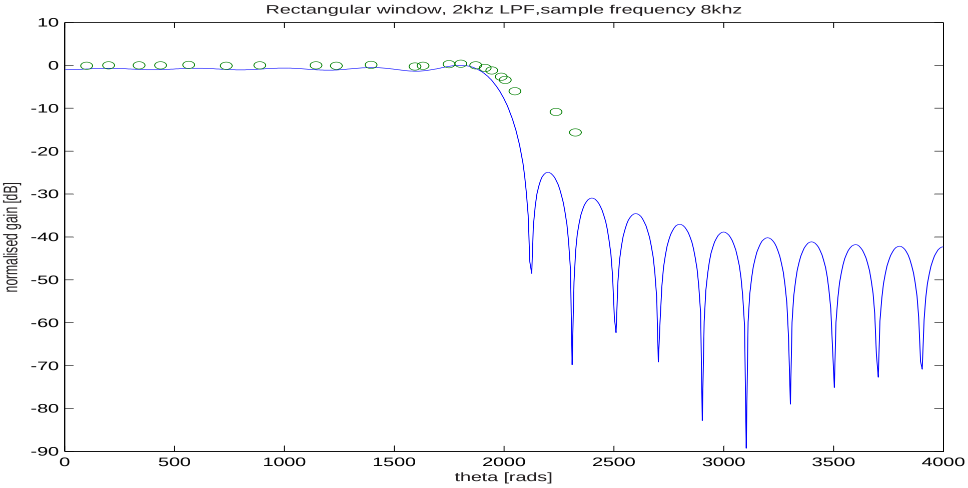

Figure 13: Rectangular Window : Comparison of theory vs measurements : f_{sample} 8kHz : gain

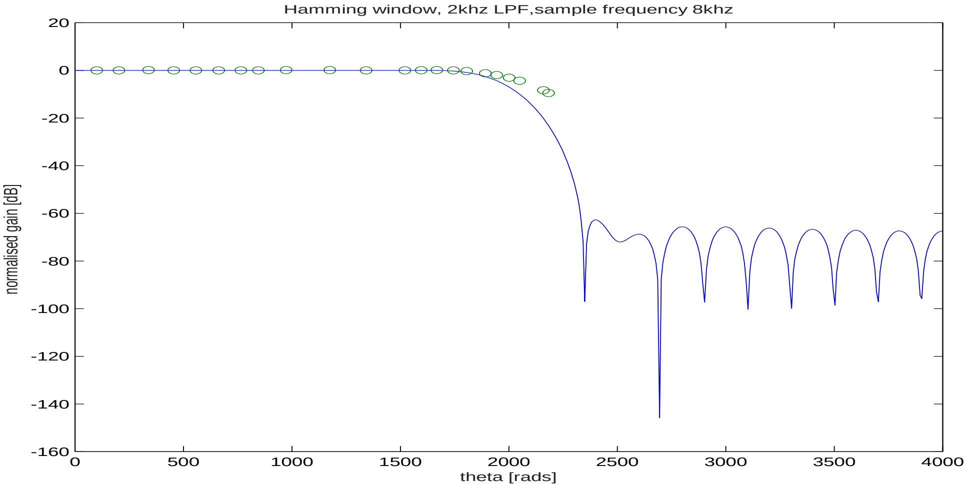

Figure 14: Hamming Window : Comparison of theory vs measurements : f_{sample} 8kHz : gain

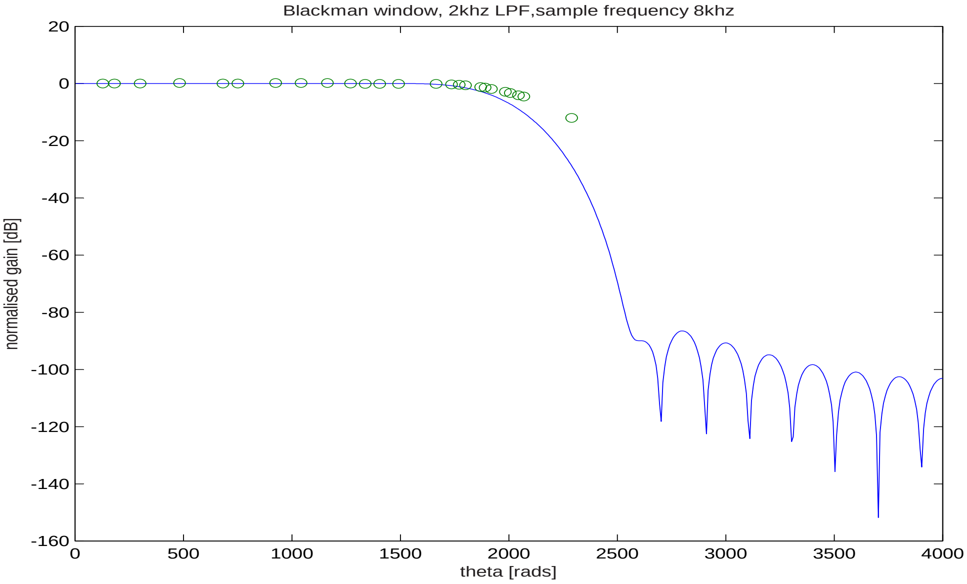

Figure 15: Blackman Window : Comparison of theory vs measurements : f_{sample} 8kHz : gain

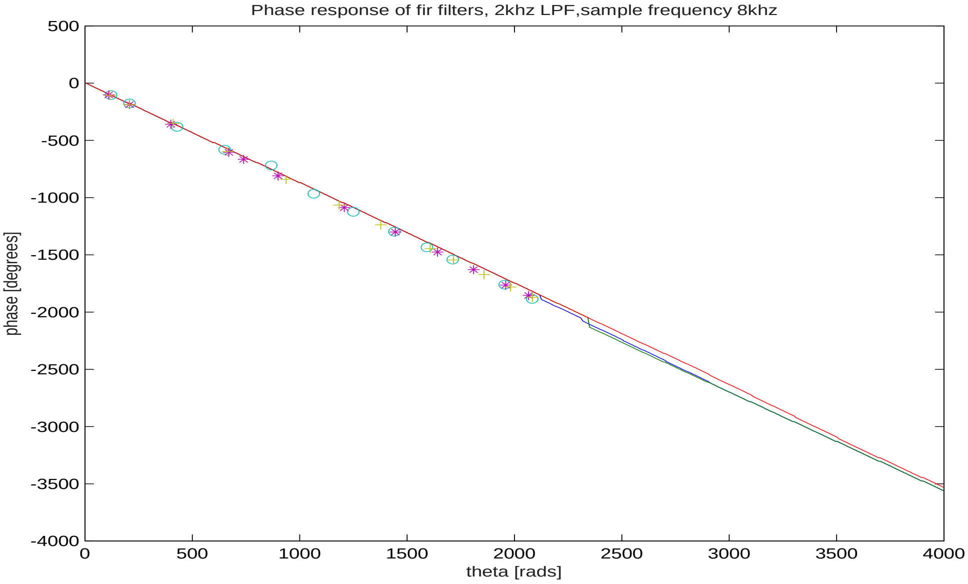

Figure 16: Empirically measured phase response : all windows, f_{sample} 8kHz

Discussion

The impulse responses of the digital filters were all inverted, but resembled the impulse response predicted throughout the assignment, and therefore corresponded closely to theory. The 48 kHz IIR filter intially returned an odd impulse response when tested, but this was subsequently rectified by greatly diminishing the gain of the filter and leaving everything else exactly the same.

Both the analogue filter, and IIR filters behaved exactly as theory predicted, with the measured readings for gain and phase fitting the theoretical curves perfectly.

The FIR filters' gain response, in isolation, looks similar to what we were expecting. The rectangular window filter had rippling occurring at the edge of the passband as expected, and this ripple on the edge of the passband was also present in the Hamming window filter, though to a far lesser extent. The Blackman window filter, on the other hand, had its gain rolling off smoothly from the passband. To this extent, the measured response reinforced the theoretical predictions.

What was unusual was that the Blackman filter had pronounced variation in the passband, in comparison to the measured gain response in the passband of the other filters and especially in comparison to the matlab Blackman window model which had the smoothest passband. What bares serious consideration is that this deviation in the passband is only 2 mV. The values that were gauged by the scope were not completely stable, and over an appreciable measuring period there was some minor fluctuation around the resting value. Oddly enough, these fluctuations were not in the first decimal place but in the full mV range. I am therefor not convinced that this accurately reflects the nature of the filter.

The lack of correlation between the theory and measured responses of the FIR filters is emphasised in the comparative plots. The FIR filters all have relatively flat passbands (neglecting rippling), and run off at the correct cut-off frequency, although they do so with a far milder slope then that predicted by the theory. Since my input signal was very weak, I had trouble attaining measurements beyond the -3dB point, as the filtered response was almost completely attenuated, and therefore failed to obtain a measurement lying on the lobes. I attribute this to the incredibly low voltage of the signal I was supplying the filter with. There was a narrow line to walk, with too large a signal overloading the chip and distorting the responses, and too small a signal making gathering readings difficult. I chose to err on the extremely weak side, and relied on the incredible senses of the oscilloscope to visual measure the signal response.

I initially ignored the unfiltered signal offered by the chip, and compared the frequency response of the filtered signal directly to the input. This was fine for the gain response of the filters although it neglected phase shifting effects inherent to the chip. This was remedied by repeating all the phase measurements for the FIR filters, and these phase measurements complied exactly with theory, lying exactly on the predicted phase line basically shared by all three FIR filters

I was amazed by the correlation between the predicted responses and measured responses. I have come to expect real world complications to introduce all manner of errors and lead to deviations away from the models. It was incredible to derive the transfer function from the analogue filter via analyse, locate the poles of this function via minor algebra, transform these poles and then to obtain the discrete transfer functions for the IIR filters. This transfer function then offered the coefficients required by the assembler code in order to implement the IIR filter. In retrospect it is a remarkably simple process to digitise existing analogue filters, and with a high sample frequency the filter will have almost identical characteristics.

Conclusion

There was incredible consistency between the theoretical and measured frequency response of the filters. The analogue filter and IIR filters responded exactly as predicted. The FIR filters followed the predicted phase perfectly, but deviated from predictions of their gain response at the cut-off frequency. This deviation is most likely attributable to the small input signal supplied to the filter at the time of investigation, and not to the design of the filter itself.

2 Bibliography

Williams, A.B. (1981), Electronic Filter Design Handbook,McGraw-Hill Book Company
Jonas, J (2005a), Digital Signal Processing,Rhodes Department of Physics & Electronics Jonas, J (2005b), The Bilinear Transformation,Rhodes Department of Physics & Electronics

3 Appendix 1 : IIR CODE

```
nsec equ 2 ;␣2␣pole␣filter

igain equ 0.0008637875 ;␣initial␣gain␣supplied␣with␣code,␣and␣results␣in␣ideal␣functionali
;
org x:  ;␣location␣of␣filter␣state␣variables␣in␣x:
state bsm 2*nsec,0 ;

org y:  ;␣location␣of␣filter␣coefficients␣in␣y:
buffer M,4*nsec

;truncated␣coefficients

;48000
;P2␣+␣P3␣=␣1.7123
;P2*P3␣=␣0.7720
;P1␣=␣0.7685

The␣assignment␣explored␣the␣design␣and␣modelling␣of␣an␣analogue␣filter␣and␣both␣an␣FIR␣and
;8000
;P2␣+␣P3␣=␣0.3190
;P2*P3␣=␣0.3461
;P1␣=␣0.1202

;Use␣full␣coefficients␣in␣filters
;48000␣&␣0.76850344092285␣&␣␣1.71225748948494␣&␣␣0.77195859080503\\

;halve␣calculated␣values
;48000␣0.38425172046143␣␣␣0.85612874474247␣␣␣0.38597929540252
;conjugate␣poles
coef dc +0.3859792954 ;␣Denominator␣z^-2
dc -0.8561287447 ;␣Denominator␣z^-1
dc +0.5000000000 ;␣Numerator␣z^-2
dc $7fffff ;␣Numerator␣z^-1␣(Biggest␣number␣less␣then␣1)

;real␣pole
dc ␣0.0000000000 ;␣Denominator␣z^-2
dc -0.3842517204 ;␣Denominator␣z^-1
dc ␣0.0000000000 ;␣Numerator␣z^-2
dc +0.5000000000 ;␣Numerator␣z^-1

;8000
;same␣as␣above␣only␣with␣different␣coefficients

endbuf

org p:

;IIR␣setup␣just␣returns
```

```
IIRsetup
rts

IIR
ori #$08,mr ;␣set␣x2␣scaling␣mode
move #state,r0 ;␣point␣to␣filter␣state
move #coef,r4 ;␣point␣to␣filter␣coefficients
move a,y0
move #igain,y1
;mpy␣complete␣multiplications␣and␣2␣moves␣in␣one␣cycle
mpy y0,y1,a␣␣x:(r0)+,x0␣y:(r4)+,y0
do #nsec,endIIR
;multiply␣and␣accumulate
mac -x0,y0,a␣x:(r0)-,x1␣y:(r4)+,y0
macr -x1,y0,a␣x1,x:(r0)+␣y:(r4)+,y0
mac x0,y0,a␣␣a,x:(r0)+␣␣y:(r4)+,y0
mac x1,y0,a␣␣x:(r0)+,x0␣y:(r4)+,y0
endIIR
rnd a
andi #$f7,mr ;␣reset␣scaling␣mode
rts
```

4 Appendix 2 : FIR CODE

```
ntap equ 41

org x:
cycbuf bsm ntap,0

org y:
buffer M,ntap
;So␣follow␣the␣FIR␣coefficients␣which␣are␣dependent␣on␣our␣windowing␣method
;Blackman␣filter
weights dc 0
dc -0.0001/1.001
dc 0
dc 0.0008/1.001
dc 0
dc -0.0028/1.001
dc 0
dc 0.0071/1.001
dc 0
dc -0.0154/1.001
dc 0
dc 0.0299/1.001
dc 0
dc -0.0546/1.001
dc 0
dc 0.0985/1.001
dc 0
dc -0.1936/1.001
dc 0
dc 0.6302/1.001
dc 1/1.001
dc 0.6302/1.001
dc 0
dc -0.1936/1.001
dc 0
dc 0.0985/1.001
dc 0
dc -0.0546/1.001
dc 0
dc 0.0299/1.001
dc 0
dc -0.0154/1.001
dc 0
dc 0.0071/1.001
dc 0
dc -0.0028/1.001
dc 0
dc 0.0008/1.001
dc 0
dc -0.0001/1.001
dc 0

endbuf

org p:
FIRsetup
move #cycbuf,r0
move #weights,r4
move #ntap-1,m0
move m0,m4
rts

FIR move a,x:(r0)
clr a x:(r0)+,x0 y:(r4)+,y0
rep #ntap-1
mac x0,y0,a x:(r0)+,x0 y:(r4)+,y0
macr x0,y0,a (r0)-
rts
```